Polymer 51 (2010) 2426–2434

Contents lists available at ScienceDirect

Polymer

journal homepage: www.elsevier.com/locate/polymer

Influence of chemical structure on enzymatic degradation of single crystals of PCL-*b*-PEO amphiphilic block copolymer

Ni Jiang [a,d], Shidong Jiang [b], Yi Hou [c], Shouke Yan [b], Guangzhao Zhang [c], Zhihua Gan [a,*]

[a] CAS Key Laboratory of Engineering Plastics, Joint Laboratory of Polymer Sciences and Materials, Institute of Chemistry, Chinese Academy of Sciences (CAS), Beijing 100190, China
[b] College of Materials Science and Engineering, Beijing University of Chemical Technology, Beijing 100029, China
[c] Department of Chemical Physics, University of Science and Technology of China, Hefei 230026, China
[d] Graduate School of Chinese Academy of Sciences, Beijing 100049, China

ARTICLE INFO

Article history:
Received 24 June 2009
Received in revised form
24 March 2010
Accepted 27 March 2010
Available online 7 April 2010

Keywords:
Amphiphilic block copolymer
Single crystal
Enzymatic degradation

ABSTRACT

Solution-grown lamellar single crystals of PCL homopolymer and amphiphilic block copolymers of PCL-*b*-PEO-*b*-PCL and PCL-*b*-PEO-FG (functional groups FG = NH_2, OCH_3) were prepared by self-seeding procedures. The crystal structure and morphology of these single crystals were mainly studied by means of transmission electron microscopy (TEM) and atomic force microscopy (AFM). The results indicated that the shorter PEO blocks as well as the functional groups bonded to the end of PEO block are in an amorphous state and located in the surface of single crystals. The enzymatic degradation of single crystals prepared from these homopolymer and amphiphilic block copolymers has been well-studied to demonstrate the effects of chemical structure on degradation behavior. The single crystals showed similar morphologies before enzymatic degradation but very different surface character after enzymatic degradation. Such differences resulted from the PEO block and functional end groups. The results of this work indicated the important role of chemical structure in determining biodegradation behavior.

1. Introduction

In recent years, biodegradable polymers have gained more and more interests for their great potential in environmental protection and biomedical fields [1–4]. For example, in the aspect of tissue engineering, poly(ϵ-caprolactone) (PCL) [5], polylactide (PLA) [6] and poly(D,L-lactide-co-glycolic acid) (PLGA) [7] were fabricated into microcarriers [8] for cell attachment and growth. These microcarriers degraded gradually in the course of cell expansion and proliferation *in vivo* [9]. Therefore, they don't need separation procedure for cell collection from microcarriers, and thus the microcarrier/cell hybrids can be delivered directly into implantation sites as scaffolds. However, most biodegradable polymers are hydrophobic and lacking of cell affinity, which restrict their applications. One method to solve this problem is to modify the surface property of microcarriers by introducing functional groups such as amino group into biodegradable polymer chains. These functional groups facilitate microcarriers to conjugate bioactive molecules and subsequently to improve the affinity with cells [10]. In addition, hydrophilic poly(ethylene oxide) (PEO) is of great interest in biomedical field due to its resistibility to nonspecific adsorption of protein, nontoxicity, absence of antigenicity and immunogenicity [11]. The PEO with low molecular weight can be thoroughly excreted through kidney [12]. In consideration of these advantages, introduction of hydrophilic PEO block with different functional groups into backbone chains of biodegradable polymers will improve both hydrophilicity and affinity to cells.

At the same time when we do chemical and physical modification to biodegradable polymers for more demanding applications, the change of chemical structures (e.g., introducing hydrophilic components and functional groups) of biodegradable polymers may greatly affect their crystallization and biodegradability, where the latter is the most essential property of biodegradable polymers for application. So it is of great significance to demonstrate the influence of chemical structure on crystallization and biodegradation behavior of amphiphilic block copolymers.

The crystallization and biodegradation behavior of PCL-*b*-PEO block copolymers have been widely investigated. Even though both PCL and PEO are crystallizable polymers, their crystallizations are mutually influenced by and depend on their relative length. Only the longer block is crystallizable when its length is 3 times or more than the another one in molar ratio [13]. The isothermal crystallization and melting behavior of PCL-*b*-PEO diblock copolymers were studied and the conclusion was that only the PCL block is crystallizable when the PEO content is lower than 20% [14]. At a fixed

* Corresponding author. Tel./fax: +86 10 62529194.
E-mail address: zhgan@iccas.ac.cn (Z. Gan).

0032-3861/$ – see front matter © 2010 Elsevier Ltd. All rights reserved.
doi:10.1016/j.polymer.2010.03.058

length of PEG block, the crystallization temperature of PCL block rises gradually from 1 to about 35 °C with increasing length of PCL block, while that of PEG block drops from 36 to −6.6 °C [15]. PCL-*b*-PEO-*b*-PCL triblock copolymer with PCL/PEO weight ratio as about 20/1 was investigated, and the PCL block crystallized quickly, and then forced the noncrystallized PEO block to form a tighter structure (helical conformation) from trans to zigzag conformation [16].

The enzymatic degradation of polymeric materials has been extensively studied in the form of films [17–21], nanoparticles [22,23], micelles [24] and microspheres [25] in order to elucidate degradation mechanism. These studies revealed that the degradation occurred first in an amorphous region and subsequently in crystalline region, and the degradation rate was strongly affected by the degree of crystallization [18,26]. Many studies have also focused on the biodegradation of PEO-*b*-PCL block copolymers [2,21,22], but the effects of chemical structure especially the functional groups along the backbone chains on biodegradation are not yet clear.

Polymer single crystals are good model substrates to elucidate the mechanism of enzymatic degradation of crystalline polymeric materials. The enzymatic degradation mechanism of single crystals of PCL [1], poly(ethylene succinate) (PES) [27] and poly(3-hydroxylbutyrate) (P(3HB)) were studied [28]. It was found that the enzymatic degradation progressed from the edges of single crystals without decreasing the lamellar thickness and molecular weights. While for the alkaline hydrolysis of poly(L-lactic acid) (PLLA) single crystals, the biodegradation firstly occurred in the loosely chain-packing region, and then gradually progressed from both crystal edges and tight chain-packing region of crystal surface [29]. For amphiphilic block copolymers, the surface behavior of single crystals is affected by the chemical structure, glass transition temperature of each block [30], surface energy [31], compositions [15] and solvent. The surface composition of single crystal can be controlled through changing the relative length of block chains. For PCL-*b*-PEO block copolymers with shorter PEO segment, the PEO chains are hard to crystallize and will be excluded from the lamella of PCL and located in the surface of single crystals. If a specific functional group is connected to PEO block as terminal group, it will locate in the surface of single crystal. What's more, a proper solvent may be propitious for the crystallization of a particular block, so it will also affect the surface composition of single crystal [30]. Therefore, single crystal will provide us a suitable model to conveniently study the influences of hydrophilic PEO block and specific functional groups on biodegradation of hydrophobic PCL block.

In this study, in order to obtain more insight into the influences of chemical structure on biodegradation behavior of amphiphilic block copolymers with functional groups in the terminal of hydrophilic segment, we prepared single crystals from homopolymer PCL, amphiphilic diblock copolymers PCL-*b*-PEO (denoted as PCL-*b*-PEO-FG, where FG is functional group), and amphiphilic triblock copolymers PCL-*b*-PEO-*b*-PCL for the study of biodegradation behavior. Transmission electron microscopy, wide-angle X-ray diffraction, atomic force microscopy, X-ray photoelectron spectroscopic and time-of-flight secondary ion mass spectrometry were employed for the characterization of polymer single crystals before and after enzymatic degradation.

2. Experimental section

2.1. Materials

PCL homopolymer (Aldrich), dihydroxyl PEO with molecular weight of 2000 (PEO_{2k}) (Aldrich) and monomethyl ether of PEO_{2k} (CH_3O-PEO, Aldrich) were purified by precipitating in an excess of methanol from their chloroform solution. The block copolymer PCL_{22k}-*b*-$PEO_{0.55k}$-NH_2 (the subscript denotes the number-average molecular weight of corresponding block) was synthesized in our group according to the previously reported procedure [9]. The diblock copolymers PCL_{10k}-*b*-PEO_{2k}-OCH_3, PCL_{20k}-*b*-PEO_{2k}-OCH_3 and triblock copolymer PCL_{10k}-*b*-PEO_{2k}-*b*-PCL_{10k} were synthesized by ring-opening polymerization of ϵ-CL with monohydroxyl CH_3O-PEO-OH and dihydroxyl HO-PEO-OH as macroinitiator and stannous octoate as catalyst [32]. The molecular weight distribution of all resultant polymers were in the range of 1.1–1.3, determined by gel permeation chromatography.

2.2. Preparation of lamellar single crystals

The single crystals of PCL-PCL-*b*-PEO-*b*-PCL and PCL-*b*-PEO-FG were grown from their dilute solution in *n*-hexanol [1]. The solution was heated to 110 °C and maintained for 15 min, then slowly cooled to 40 °C at a rate of 10 °C/h for isothermal crystallization overnight. Then the solution was reheated again to an elevated temperature for producing seeds via which the more perfect single crystals could be obtained by lowering the temperature again for isothermal crystallization overnight. After repeating this cycle for two times, the solution was slowly cooled to room temperature, and the crystals were collected by centrifugation and washed several times with methanol.

2.3. Morphological observation by AFM

Drops of single crystal suspension were deposited on cleaned Si wafer and allowed to dry. Tapping-mode atomic force microscopy (AFM) images were obtained at room temperature by using a NanoScope III MultiMode AFM (Digital Instruments). Phase and height images were recorded simultaneously using the retrace signal. Si tips (TESP) with a resonance frequency of approximately 300 kHz and a spring constant of about 40 Nm^{-1} were used, and the scan rate was in the range of 0.7–1.2 Hz with a scanning density of 512 lines/frame.

2.4. Surface analysis by XPS and ToF-SIMS

The crystal suspension was deposited on a clean 15 mm × 15 mm Si wafer and allowed to dry. X-ray photoelectron spectroscopy (XPS) data were obtained with an ESCALab220i-XL electron spectrometer from VG Scientific using 300 W Al Kα radiation. The base pressure was about 3×10^{-9} mbar. The binding energies were referenced to the C_{1s} line at 284.8 eV from adventitious carbon. The takeoff angle (TOA) was defined as the angle between the horizontal axis of the surface and the axis of the analyzer lens system [31]. The TOA of 90° employed lead approximately to sampling depths of ca 2–10 nm.

Time-of-flight secondary ion mass spectrometry (ToF-SIMS) has been widely used to study polymer surface structures [18,33]. More recently, ToF-SIMS imaging has been used to investigate the surface morphologies. In this work, ToF-SIMS was carried out on a Physical Electronics PHI 7200 ToF-SIMS spectrometer to acquire the surface chemical images of copolymer in both positive and negative modes by using a $69Ga^+$ beam at 25 kV. To obtain high-resolution spatial images, an ion pulse width of about 50 ns was used. The total ion dose for each image acquisition was lower than 4×10^{12} ions/cm^2. Charge compensation was realized by low-energy (0–70 eV) flooding electrons being pulsed out of phase of the primary ion beam. The scanned area was 200 μm × 200 μm, and the total ion dose for each spectrum acquisition was <1012 ions/cm^2.

2.5. Morphological and structural analysis by TEM and WAXD

Drops of the single crystal suspension were deposited on carbon-coated grids, allowed to dry, and then shadowed with Pt–Pd alloy. For electron diffraction purpose, the dried crystals were used directly without further treatments. The transmission electron microscopy (TEM) observations were performed on a JEM GEOL-100CX operated at 100 kV. Bright-field (BF) phase contrast micrographs were obtained by defocus of the objective lens.

Wide-angle x-ray diffraction (WAXD) was used to determine the crystal structures of PCL-*b*-PEO block copolymers as well as PEO and PCL homopolymers. The PEO, PCL and PCL_{20k}-*b*-PEO_{2k}-OCH_3 films were prepared by hot compression between two Teflon films with another 0.15 mm thick Teflon film as spacer. All the samples were compressed at 80 °C for 4 min, and then transferred quickly into oven at 40 °C for isothermal crystallization. The WAXD patterns of these films were recorded at room temperature on a Rigaku D/Max-2500 diffractometer with a nickel-filtered Cu Ka radiation (wavelength $\lambda = 0.154$ nm, 40 kV and 110 mA) in the 2θ range of 5–40° with a scanning step of 1°.

2.6. Enzymatic degradation of single crystals

Degradation of single crystals was carried out in phosphate buffer solution (PBS) with the presence of lipase from *Pseudomonas cepacia* (Lipase PS) at 37 °C in a shaker with a speed of 100 rpm. For investigation of morphological changes by AFM, drops of single crystal suspension were deposited on clean Si wafer, allowed to dry and then put it into an ampoule. 2 ml PBS containing 0.2 mg lipase was added into the ampoule to start the biodegradation. After 10 min, the ampoule was taken out from the shaker and washed with deionized water for three times to remove the lipase. After then, these Si wafer with single crystals on the surface were lyophilized and the surface morphology was examined by AFM.

2.7. QCM-D measurements

Polymer thin films and single crystals on a QCM-D were prepared by spin-casting of polymer solution in THF solutions (0.1 wt%) and polymer single crystal suspensions on a spin-coater (CHEMAT, KW-400) at 3000 rpm in air. The thickness of the film was controlled by polymer concentration while the single crystals were controlled by pretty much of the same frequency shifts which have been measured by QCM-D in air before and after spin-casting. A measurement of the degradation was initiated by switching the liquid exposed to the gold-coated quartz resonator from a 0.1 M phosphate buffer solution (PBS, pH 7.0) to an enzyme solution. The total volume used for replacement was about 2 mL. Δf and ΔD values from the fundamental were discarded because they were usually noisy due to insufficient energy trapping [34]. All the experiments were performed at 30 °C.

3. Results and discussion

3.1. Morphology and structure of lamellar single crystals

In this work, single crystals of PCL, PCL_{10k}-*b*-PEO_{2k}-*b*-PCL_{10k}, PCL_{20k}-*b*-PEO_{2k}-OCH_3 and PCL_{22k}-*b*-$PEO_{2.2k}$-NH_2 were grown from *n*-hexanol by a self-seeding method. Since the equilibrium dissolution temperature of PCL_{20k} in *n*-hexanol is much higher than PEO_{2k}, while PEO_{2k} is soluble even at room temperature, it is hard for PEO to form seeds. Therefore, the self-seeding method and the used *n*-hexanol solvent are propitious for the crystallization of PCL blocks in copolymer.

The electron micrographs of single crystals were shown in Fig. 1. All polymers were found to grow lamellar crystals with multilayers developing from screw dislocations. The single crystal of PCL homopolymer was of hexagonal shape (Fig. 1a), while the other single crystals of PCL-containing block copolymers were of

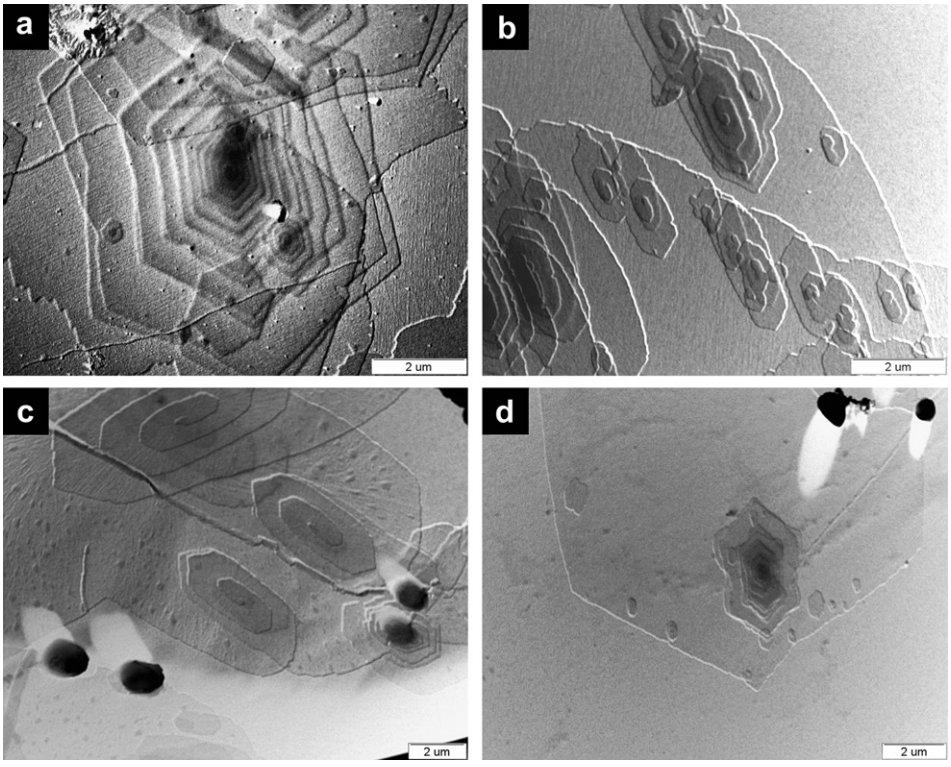

Fig. 1. Electron micrographs of single crystals after shadowing with Pt–Pd alloy. (a) PCL. (b) PCL_{10k}-*b*-PEO_{2k}-*b*-PCL_{10k}. (c) PCL_{20k}-*b*-PEO_{2k}-OCH_3. (d) PCL_{22k}-*b*-$PEO_{2.2k}$-NH_2.

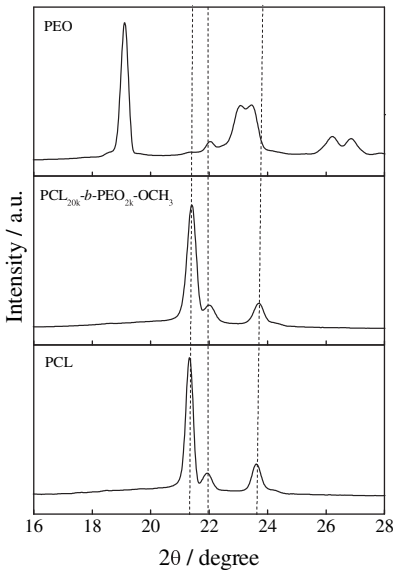

Fig. 2. WAXD patterns of the PEO, PCL and PCL_{20k}-*b*-PEO_{2k}-OCH_3 block copolymer after isothermal crystallization at 40 °C by cooling rapidly from the melt.

elongated hexagonal shapes (Fig. 1b–d). These single crystals have similar shapes to PCL but different ones from the square shape of PEO [35], suggesting that the copolymers have the same crystal structure to PCL homopolymer. The morphological results of these single crystals were in agreement with other report [35].

In order to confirm the single crystal structure of block copolymers and to answer where the PEO segments existed in single crystals of amphiphilic block copolymers, the WAXD of PEO, PCL and PCL_{20k}-*b*-PEO_{2k} films and the electron diffraction of selected domain of all single crystals were performed. From the WAXD pattern as shown in Fig. 2, it was found that the block copolymers show the diffraction peaks with the same location to PCL homopolymer, but different from those diffraction peaks of PEO homopolymer. These results indicated that only the PCL block in the PCL_{20k}-*b*-PEO_{2k} block copolymer can crystallize with this composition even though the corresponding homopolymers of both PEO and PCL blocks are crystallizable polymers. The electron diffractions of selected domain of all single crystals were shown in Fig. 3. It was found that the PCL single crystals show strong (110) and (200) reflections, implying an orthorhombic packing and a perfect crystallographic orientation along *c* axis (the chain direction) which is perpendicular to the plane of single crystal. While the monoclinic PEO single crystals show two pairs of strong diffraction spots which are perpendicular to each other and contributed to the (120) planes [35]. For single crystals of all amphiphilic block copolymers in this work, they showed strong electron diffraction spots which are the same to those diffraction spots of PCL single crystals (see Fig. 3b–d). Therefore, based on the results from WAXD and electron diffraction, it has been concluded that for three copolymers of PCL_{10k}-*b*-PEO_{2k}-*b*-PCL_{10k}, PCL_{20k}-*b*-PEO_{2k}-OCH_3 and PCL_{22k}-*b*-$PEO_{2.2k}$-NH_2, only the longer PCL blocks are folded to form single crystals, the shorter PEO blocks are excluded from PCL lamella and located in the surface of single crystals as an amorphous state, even though both PCL and PEO blocks are crystalline polymers.

The AFM phase images of all single crystals of PCL homopolymer and PCL-containing block copolymers were shown in Fig. 4. All single crystals clearly showed multi-layered lamellar crystals with a thickness of about 10 nm. With further observation, six sectors in single crystal layer for all polymer single crystals could be seen. Among the six sectors, four sectors had emanative lines from the screw dislocation center while the other two did not. This morphological phenomenon resulted from the PCL chain folding directions on the growing faces. The results also indicated that the amorphous PEO layer on the surface of single crystals of block copolymers is thin and does not conceal the folding direction of PCL blocks.

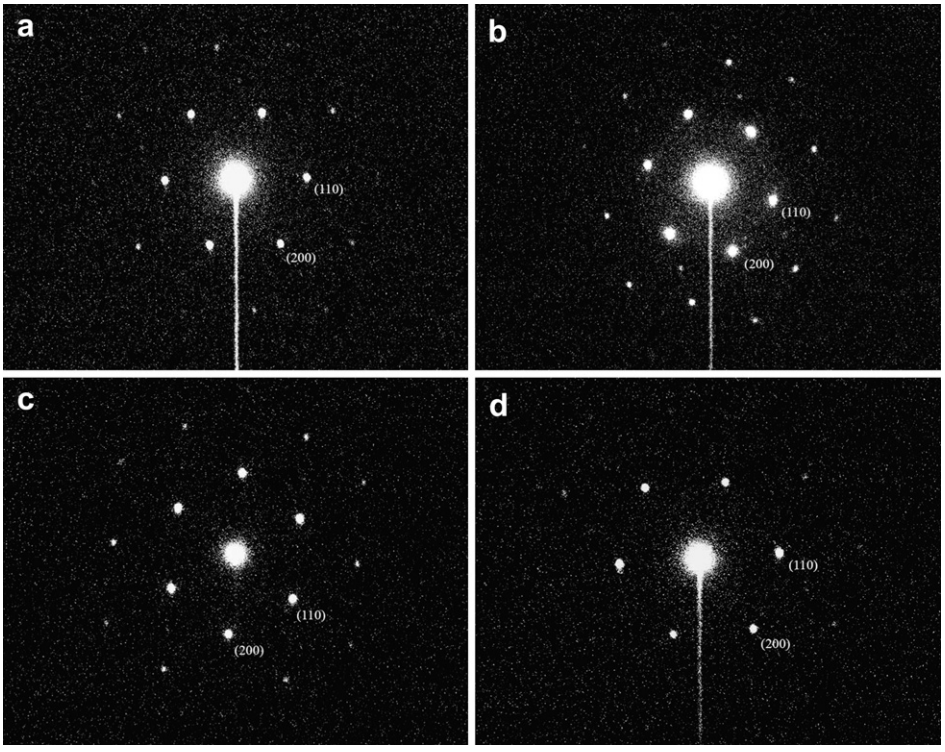

Fig. 3. Electron diffraction patterns of single crystals of (a) PCL, (b) PCL_{10k}-*b*-PEO_{2k}-*b*-PCL_{10k}, (c) PCL_{20k}-*b*-PEO_{2k}-OCH_3, (d) PCL_{22k}-*b*-$PEO_{2.2k}$-NH_2.

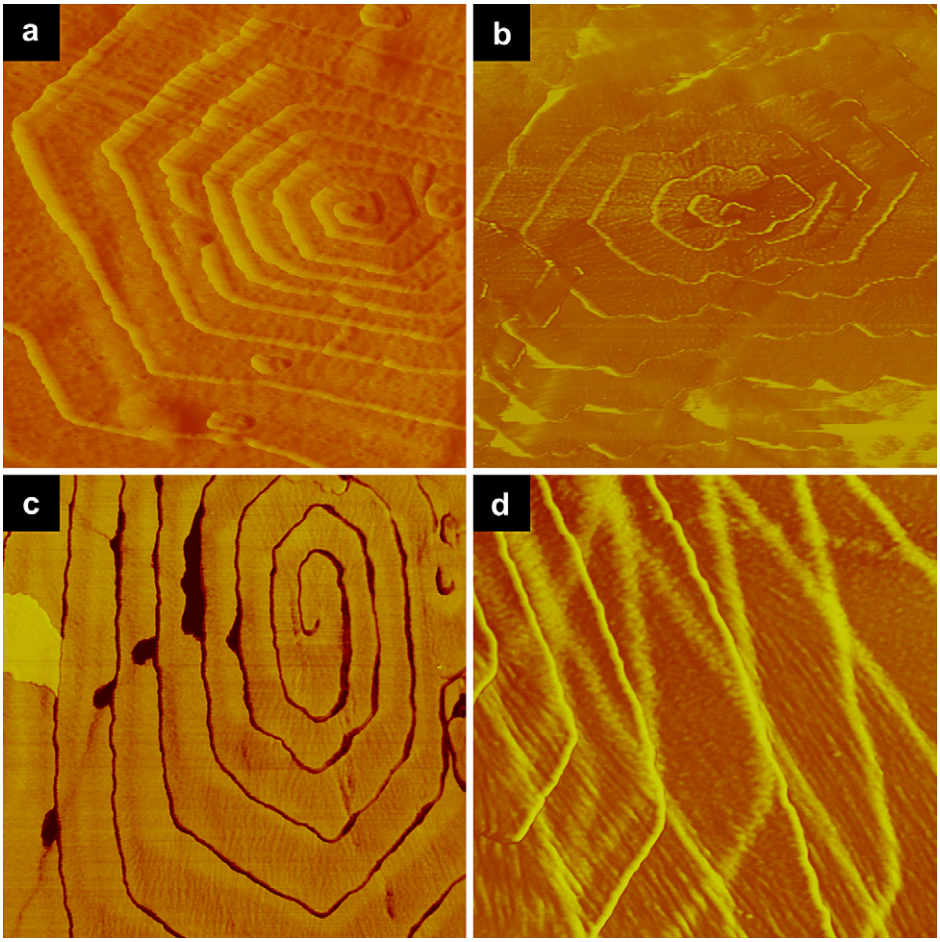

Fig. 4. AFM phase images of single crystals of (a) PCL, (b) PCL_{10k}-*b*-PEO_{2k}-*b*-PCL_{10k}, (c) PCL_{10k}-*b*-PEO_{2k}-OCH_3 and (d) PCL_{22k}-*b*-$PEO_{2.2k}$-NH_2. The size of each picture is 2.5 μm × 2.5 μm.

3.2. Surface properties of lamellar single crystals

For the single crystals grown from block copolymers of PCL_{20k}-*b*-PEO_{2k}-OCH_3 and PCL_{22k}-*b*-$PEO_{2.2k}$-NH_2, the electron diffraction and WAXD results have indicated that the PEO block are in an amorphous state in the surface of single crystals, it could be imaged that the terminal groups such as NH_2 and OCH_3 which are bonded to the end of PEO block should be existed in the surface layer of single crystals. If so, not only the surface of single crystal could be controlled, but also the interaction with biological molecules would be influenced by the functional terminal groups. To confirm this result, with single crystal of PCL_{22k}-*b*-$PEO_{2.2k}$-NH_2 as an example, angular dependent X-ray photoelectron spectroscopy (XPS) and time-of-flight secondary ion mass spectrometry (ToF-SIMS) were used to quantify the distribution of amino groups in single crystals.

Table 1
XPS analysis of surface composition on single crystals prepared by PCL_{22k}-*b*-$PEO_{2.2k}$-NH_2.

Take-off angle (degree)	Molar ratio of carbon to nitrogen (C:N)	
	Surface[a]	Bulk[b]
20	149.4	1257.9
30	59.9	
45	87.6	

[a] Determined by XPS measurement.
[b] Calculated by composition of PCL_{22k}-*b*-$PEO_{2.2k}$-NH_2 block copolymer.

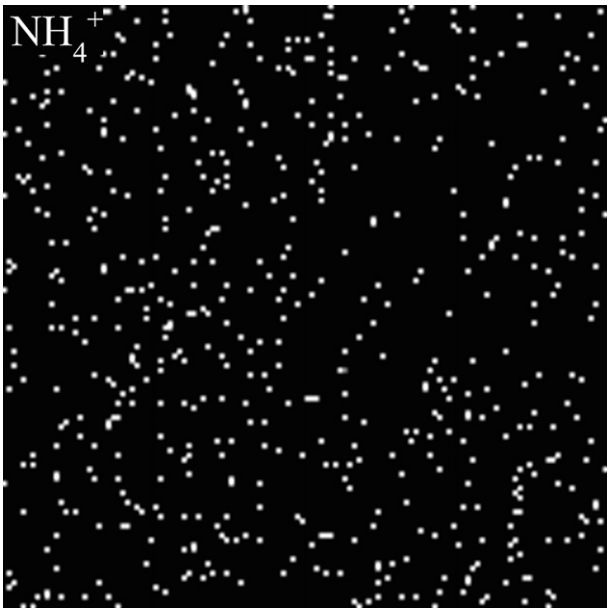

Fig. 5. The ToF-SIMS image of PCL_{22k}-*b*-$PEO_{0.55k}$-NH_2 single crystals.

For XPS measurement, the penetration depth of X-ray from surface into interior of sample depends on the takeoff angle (TOA). The penetration depth decreases with the decreasing of TOA. To analyze the distribution of amino groups (NH_2) in single crystals, the XPS measurements were performed at various TOA to determine the molar ratios of carbon to nitrogen (C/N ratio), and the results were summarized in Table 1.

Suppose the amino groups distribute homogeneously in the bulk of PCL_{22k}-*b*-$PEO_{2.2k}$-NH_2 single crystals, the C/N ratio is calculated as 1257.9 based on the composition of copolymers. However, the XPS results in Table 1 showed that the C/N ratio in the surface layer of single crystal from the most upper to the inner are orderly as 149.4, 59.9 and 87.6, which are much lower than that of the calculated 1257.9, implying the high contents of N atom in the surface layer of single crystals. Therefore, the results in Table 1 clearly indicated that the amino groups are dominantly distributed in the surface amorphous layer of single crystals.

The data in Table 1 also demonstrate that the concentration of amino groups is the greatest when the TOA is 30° but not 20°. The possible reason for the nonhomogeneous distribution of amino

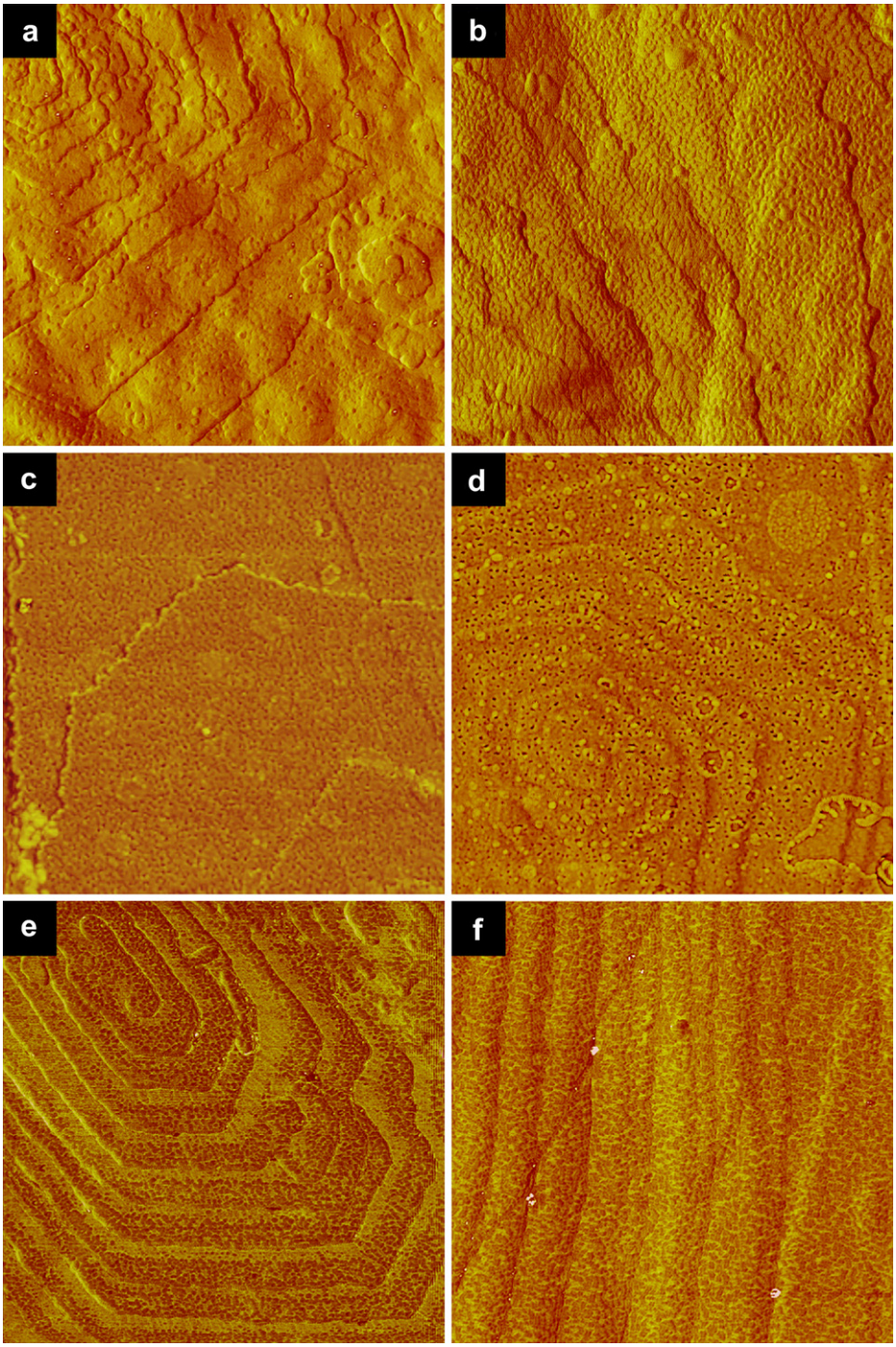

Fig. 6. AFM phase images of single crystals of (a) PCL, (b) PCL_{10k}-*b*-PEO_{2k}-*b*-PCL_{10k}, (c) PCL_{22k}-*b*-$PEO_{0.55k}$-NH_2, (d) PCL_{22k}-*b*-$PEO_{2.2k}$-NH_2, (e) PCL_{10k}-*b*-PEO_{2k}-OCH_3 and (f) PCL_{20k}-*b*-PEO_{2k}-OCH_3 after enzymatic degradation. The size of each picture is 2.5 μm × 2.5 μm.

groups along the depth direction (i.e., the *c*-axis direction of single crystal) is that the hydrophilic segment has higher surface energy, which is disadvantageous for the hydrophilic amino groups to stand on the upper surface. The NH_4^+ images of the single crystal surface can be used to determine the spatial distribution of the amino groups because the NH_4^+ are characteristic positive ions of the copolymer. ToF-SIMS NH_4^+ images for PCL-*b*-PEO-NH_2 copolymer were displayed in Fig. 5. The white spots distributed homogenously across the surface, indicating the homogenous distribution of amino groups in the surface plane of in the surface plane of single crystal (i.e., the plane perpendicular to the *c*-axis direction of single crystal). Therefore, it could be concluded that the amino groups are distributed dominantly in the surface layer of single crystals of PCL_{22k}-*b*-$PEO_{2.2k}$-NH_2. Based on this conclusion, it could be pointed out that this is a useful method to control the surface chemical and amphiphilic properties of single crystals by changing the composition and terminal groups of amphiphilic block copolymers. Such kind of method to control surface property could be useful to adjust the interaction between biological molecules (such as protein, enzyme) and surface of polymeric nanomaterials.

3.3. Enzymatic degradation of lamellar single crystals

The AFM images of single crystals after enzymatic degradation promoted by lipase were shown in Fig. 6. It was found that the single crystals of PCL homopolymer and block copolymers show very different surface character after degradation even though their morphologies are similar before degradation. For PCL single crystals, enzymatic degradation mainly took place on the edges of lamellar crystals, resulting in the irregular edges (see Fig. 6a). This is in agreement with the report that the PCL single crystals degrade mainly from the edges of the lamella crystals where the chain-packing is loose [1]. While for copolymer single crystals, besides the lamellar edges, the surface of single crystals showed obvious changes after enzymatic degradation. The six sectors became rough and could not be seen any more (see Fig. 6b–d). In consideration of the results that the PEO blocks exist on the surface of single crystals of copolymers, it could be concluded that it is the introduction of PEO blocks that resulted in the obvious difference of surface character between PCL homopolymer and PCL-*b*-PEO copolymer single crystals after enzymatic degradation.

As we have known that the attack of the lipase onto polymer is the first step for the enzymatic degradation, water-soluble lipases undoubtedly like to adsorb on the hydrophilic surface. So for the hydrophilic surface of lamella crystals fabricated by the copolymers containing PEO chains, it is more favorable for lipase to adsorb homogeneously on the surface of single crystals, resulting in the homogeneous change of single crystal surface during enzymatic degradation process. While for PCL homopolymers, the hydrophobic surface of single crystals may not favor for lipases to adsorb on, so the degradation mainly occurred from the loose chain-packing edges.

The influences of PEO block length on the surface of copolymer single crystals after enzymatic degradation were shown in Fig. 6 (images c, d, e and f). For PCL-*b*-PEO-NH_2 copolymers with fixed PCL block length (22,000, denoted by molecular weight of block), the single crystal surface showed more obvious and dense holes after enzymatic degradation when decreasing the PEO block length from 2200 to 550 as shown in Fig. 6c and d, indicating the more obvious degradation of copolymer single crystals with shorter PEO blocks. This is because of the longer PEO block chains which occupy relatively larger space to protect PCL single crystal surface provisionally. Similar changes after enzymatic degradation were also seen for the single crystals of PCL-*b*-PEO-OCH_3 copolymers with fixed PCL block length but different PEO block length (see Fig. 6e and f).

Since the different groups were bonded to the hydrophilic PEO block, the influences of terminal groups on enzymatic degradation of copolymer single crystal were investigated. Three samples with similar composition but different chemical structures were used for this issue: PCL-*b*-PEO-*b*-PCL, PCL-*b*-PEO-NH_2 and PCL-*b*-PEO-OCH_3. Based on the previous discussion, we have known that functional groups of NH_2 and OCH_3 are distributed in the surface layer of single crystals which were fabricated from PCL-*b*-PEO-NH_2 and PCL-*b*-PEO-OCH_3, respectively, while there is no any functional group in the surface layer for PCL-*b*-PEO-*b*-PCL triblock copolymer single crystals since both the terminals of PEO block were capped by PCL blocks. The results in Fig. 6b, d and f indicated that the single crystals of PCL-*b*-PEO-OCH_3 and PCL-*b*-PEO-*b*-PCL show similar wrinkled surface property after enzymatic degradation, while the single crystals of PCL-*b*-PEO-NH_2 show homogeneous holes and islets on the surface.

The different surface changes of these copolymer single crystals after enzymatic degradation should be due to the surface properties by introducing different terminal groups into the PEO block. The amino group is polar and hydrophilic, so it shows good interaction with enzymes. While the methoxy group and PCL block (for PCL-*b*-PEO-*b*-PCL, PCL blocks could be regarded as a functional group connected to the end of PEO block) are hydrophobic, so they show different interaction with enzyme compared to amino group. Such kind of difference in hydrophilic and hydrophobic properties of NH_2 and OCH_3 terminal groups results in the different surface changes of copolymer single crystals.

The influences of surface properties on enzymatic degradation of single crystals were further investigated by QCM. The time dependence of frequency changes (Δf) of the quartz resonator

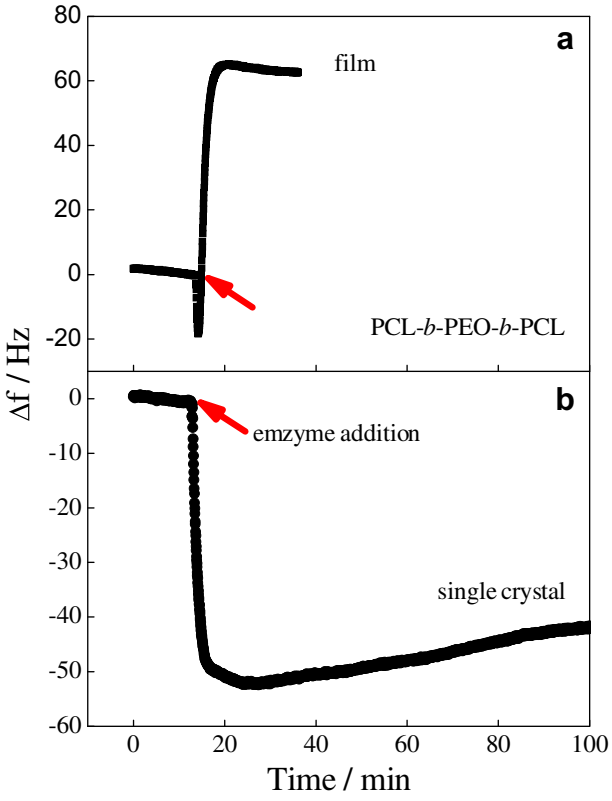

Fig. 7. The frequency shifts (Δf) of QCM during enzymatic degradation of PCL-*b*-PEO-*b*-PCL film (a) and single crystals (b) catalyzed by lipase PS, where $C_e = 0.1$ mg/ml.

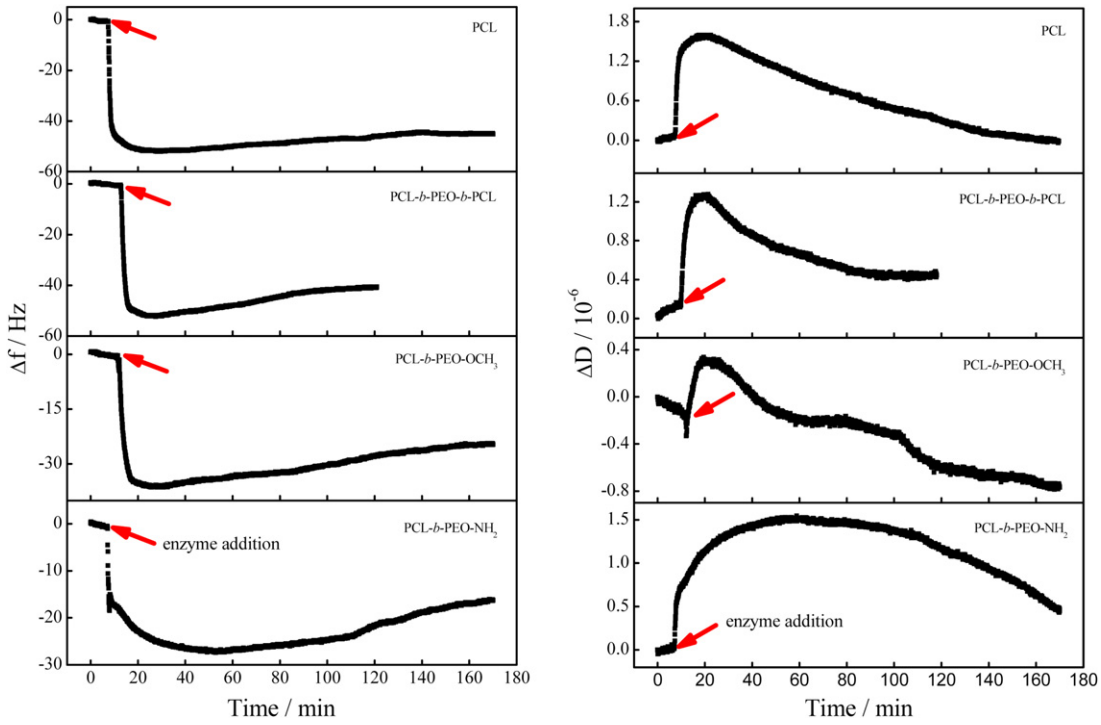

Fig. 8. The frequency shifts (Δf) and dissipation shifts (ΔD) of QCM during enzymatic degradation of single crystals catalyzed by lipase PS, where C_e = 0.1 mg/ml.

coated with PCL film and single crystals during enzymatic degradation in buffer solution was shown in Fig. 7. The frequency change can be attributed to the mass change of polymer films or single crystals. For both PCL films and single crystals, a negative frequency shift was observed after lipase was added into the buffer solution due to the adsorption of enzyme as well as the fluctuation of concentration and temperature. The following sharp increase in Δf for PCL films and slow increase in Δf for PCL single crystals clearly indicated the fast mass loss of films and slow mass loss of single crystals. The results in Fig. 7 clearly show the difference in enzymatic degradation rates of PCL films and single crystals due to their different crystallinity.

The time dependence of frequency changes (Δf) and dissipation changes (ΔD) of the quartz resonator coated with single crystals of PCL homopolymer and PCL-*b*-PEO copolymers were shown in Fig. 8. Compared to PCL film (Fig. 7a), all the single crystals no matter prepared by PCL homopolymer or PCL-*b*-PEO copolymers showed similar frequency changes (Δf) with time as shown in Fig. 8a, indicating a slower enzymatic degradation rate. Meanwhile, the dissipation changes (ΔD) for all single crystal samples showed the similar tendency with time regardless of composition and functional end groups (Fig. 8b).

The rough surface of copolymer single crystals after enzymatic degradation was shown in Fig. 6, and the looseness or thickening of a polymer layer on quartz resonator has been known to lead to the increase of dissipation. However, the results of Figs. 8b and 6 suggested that there are too many factors for the change of dissipation of polymer single crystals in the course of enzymatic degradation. As shown in Figs. 1 and 4, the stacked lamellar single crystals grew by screw dislocation. Enzymatic degradation not only resulted in the roughness of single crystal surface, but also resulted in the loss of lamellar crystals layer by layer. Compared to the surface change of lamellar crystals, the loss of one crystal lamellae resulted in the obvious change in thickness of stacked lamellar crystals. Therefore, even though the surface of single crystals became rougher after enzymatic degradation as shown in Fig. 6, the thickness change of stacked lamellar single crystals in the way of layer-by-layer played a more important role in determining the changes of dissipation.

4. Conclusion

In this work, solution-grown lamellar single crystals of PCL homopolymer, PCL-*b*-PEO-*b*-PCL and PCL-*b*-PEO-FG (FG = NH_2, OCH_3) block copolymers have been prepared by self-seeding procedures. Structural analysis of the crystals revealed that short PEO blocks are in an amorphous state located in the surface of single crystals. The functional groups such as NH_2 and OCH_3 at the end of PEO blocks are homogeneously distributed in the surface layer of single crystals. The results on enzymatic degradation of single crystals indicated the important roles of both PEO block and functional groups in affecting the different interaction between polymer and enzymes. The results of this work provide an efficient way to regulate the surface properties of polymer nanomaterials via altering the composition and functional terminal groups of amphiphilic block copolymers.

Acknowledgment

This work was supported by the National Natural Science Foundation of China (Grant no. 2047042, 50521302), the Hundreds Talents Project of Chinese Academy of Sciences.

References

[1] Iwata T, Doi Y. Polym Int 2002;51:852.
[2] He F, Li S, Vert M, Zhuo R. Polymer 2003;44:5145.
[3] Pizzoli M, Scandola M. Macromolecules 1994;27:4755.
[4] Baimark Yodthong. Polymer 2009;50:4761.
[5] Waddell RL, Marra KG, Collins KL, Leung JT, Doctor JS. Biotech Prog 2003;19:1767.
[6] Cartier L, Okihara T, Ikada Y, Tsuji H, Puiggali J, Lotz B. Polymer 2000;41:8909.
[7] Newman KD, Michael MW, Burney WM. Biomaterials 2004;25:5763.
[8] Van Wezel AL. Nature 1967;216:64.
[9] Yu GQ, Zhang Y, Shi XD, Li ZS, Gan ZH. J Biomed Mater Res A 2008;4:926.

[10] Zhu Y, Gao C, Liu X, Shen J. Biomacromolecules 2002;3:1312.
[11] Herold CB, Keil K, Bruns DE. Biochem Pharmacol 1989;38:73.
[12] Shaffer CB, Critchfield FH. J Am Pharm Assoc 1947;36:152.
[13] Floudas G. Macromolecules 1998;31:7279.
[14] Gan ZH, Jiang BZ, Zhang J. J Appl Polym Sci 1996;59:961.
[15] He C, Sun J, Deng C, Zhao T, Deng M, Chen X, et al. Biomacromolecules 2004;5:2042.
[16] Yu J, Wu P. Polymer 2007;48:3477.
[17] Doi Y, Kitamura S, Abe H. Macromolecules 1995;28:4822.
[18] Kumagai Y, Kanesawa Y, Doi Y. Makromol Chem 1992;193:53.
[19] Gan ZH, Yu DH, Zhong ZY, Liang QZ, Jing XB. Polymer 1999;40:2859.
[20] Koyama N, Doi Y. Macromolecules 1997;30:826.
[21] Canetti M, Urso M, Sadocco P. Polymer 1999;40:2587.
[22] Gan ZH, Jim TF, Jing XB, Wu C, Kuliche WK. Polymer 1999;40:1961.
[23] Piao LH, Dai ZL. Polymer 2003;44:2025.
[24] Nie T, Zhao Y, Xie Z. Macromolecules 2003;36:8825.
[25] Chen D, Chen H, Bei J, Wang S. Polym Int 2000;49:269.
[26] Hou Y, Chen J, Sun PJ, Gan ZH, Zhang GZ. Polymer 2007;48:6348.
[27] Iwata T, Doi Y. Macromolecules 2001;34:7343.
[28] Iwata T, Doi Y. Macromolecules 1997;30:833.
[29] Iwata T, Doi Y. Transaction 2001;40:193.
[30] Chen WY, Li CY, Zheng JX, Huang P, Zhu L, Ge Q, et al. Macromolecules 2004;37:5292.
[31] Mori H, Hirao A, Nakahama S. Macromolecules 1994;27:4093.
[32] Xie WY, Jiang N, Gan ZH. Macromol Biosci 2008;8:775.
[33] Lei YG, Cheung ZL, Ng KM, Li L, Weng LT, Chan CM. Polymer 2003;44:3883.
[34] Voinova MV, Rodahl M, Jonson M, Kasemo B. Phys Scr 1999;59:391.
[35] Sun JR, Chen XS, He CL, Jing XB. Macromolecules 2006;39:3717.